DALTON
FULL PAPER

Oxidative addition of chlorinated solvents (*e.g.* CH_2Cl_2 and $CHCl_3$) with rhodium(I) complexes; crystal structure of *mer*-$[Rh(py)_3(CH_2Cl)Cl_2]$

Kerry J. Bradd, Brian T. Heaton,* Chacko Jacob, Jeyagowry T. Sampanthar and Alexander Steiner

Chemistry Department, University of Liverpool, Liverpool, UK L69 7ZD.
E-mail: amf@liverpool.ac.uk

Received 10th December 1998, Accepted 9th February 1999

Common chlorinated solvents (*e.g.* CH_2Cl_2 and $CHCl_3$) readily reacted with $[Rh_2(C_8H_{14})_4(\mu\text{-}Cl)_2]$ (C_8H_{14} = cyclooctene), in the presence of a monodentate, nitrogen donor ligand (L = py or 4-Bu^{t}py), to give the oxidative addition product $[RhL_3RCl_2]$ (R = CH_2Cl, $CHCl_2$ or CH_2Ph) which for R = CH_2Cl and CH_2Ph has been shown by X-ray analysis to adopt the *mer* configuration. NMR Spectroscopic measurements (^{13}C and ^{15}N) in solution were consistent with this configuration, although these NMR data cannot unambiguously distinguish between the *mer* and *fac* isomers.

The oxidative addition reaction of aliphatic compounds containing a C–X bond (X = Cl, Br or I) by low-valent transition metal complexes is of interest because many catalytic processes involve this reaction as the key step. There are many examples of oxidative addition reactions involving molecules of the type CH_3X (X = I or Br) and numerous reports with CH_2I_2, CH_2Br_2 and CH_2ICl. Early reports of analogous reactions with the common solvents CH_2Cl_2 and $CHCl_3$ suggested that thermal[1] or photochemical[2–4] initiation was necessary. However, several reactions involving the reaction of CH_2Cl_2 with transition metal complexes under mild conditions have been documented over recent years and the group derived from CH_2Cl_2 in the resulting product can be either (i) CH_2Cl, (ii) $\mu\text{-}CH_2$ or (iii) a metal carbene species.

Examples of simple oxidative addition of CH_2Cl_2 to form chloromethyl complexes have been reported for electron-rich transition metal complexes containing mono-[5–7] or polydentate phosphine ligands,[8,9] bi- or tri-dentate nitrogen ligands,[10–12] sulfur macrocycles[13] and phosphorus–nitrogen hybrid ligands.[14–16]

Double oxidative addition reactions to two metal centres have been observed with the highly basic rhodium complexes $[Rh_2(dppe)_2(\mu\text{-}Cl)_2]$,[17] $[Rh_2(PR_3)_4(\mu\text{-}Cl)_2]$[18] ($PR_3$ = PEt_3 or PPh_2Me) and $[Rh_2(CNBu^t)_4(\mu\text{-}pz)_2]$ (pz = pyrazolate).[19]

The third type of oxidative addition reaction of CH_2Cl_2 to form a metal–carbene species has been reported to occur with the ruthenium complex $[RuH_2(H_2)_2L_2]$ [L = $P(C_6H_{11})_3$] to form $[RuCl_2(CH_2)L_2]$.[20] This is the only known example of this type of reaction and involves the double oxidative addition of CH_2Cl_2 to a single metal centre.

Some of the above work has recently been reviewed.[21]

In this paper we report the facile oxidative addition of CH_2Cl_2, $CHCl_3$ and $PhCH_2Cl$ to the rhodium(I) complex $[Rh_2(C_8H_{14})_4(\mu\text{-}Cl)_2]$ in the presence of monodentate nitrogen ligands (*e.g.* py, 4-Bu^{t}py) to form the rhodium(III) product $[RhL_3RCl_2]$ (L = py or 4-Bu^{t}py; R = CH_2Cl, $CHCl_2$ or CH_2Ph) (see Scheme 1). This is the first example of this type of reaction involving complexes containing only *monodentate* nitrogen-donor ligands.

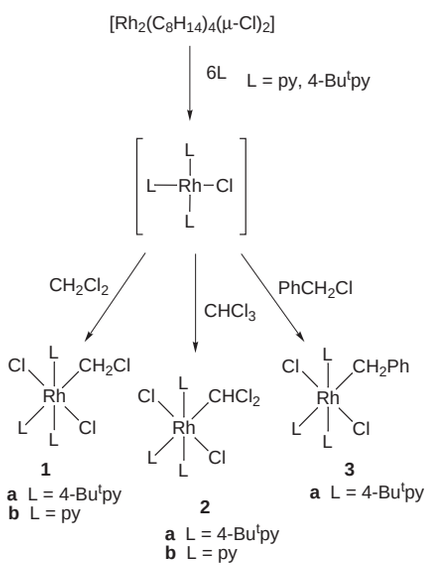

Scheme 1

Results and discussion

The reactions shown in Scheme 1 occur readily at room temperature but attempts to identify the presumed intermediate, $[RhL_3Cl]$, by carrying out spectroscopic measurements at low temperature in the absence of RCl were unsuccessful and there is no NMR spectroscopic evidence for other complexes of Rh^{I} or Rh^{III} containing co-ordinated cyclooctene. However, NMR measurements (^{13}C and ^{15}N) show that oxidative addition of RCl occurs to give $[RhL_3RCl_2]$ but it proved impossible to distinguish between isomers **A** and **B** from spectroscopic measurements. However, in the case of $[Rh(py)_3(CH_2Cl)Cl_2]$ **1b**† it was possible to isolate crystals for X-ray diffraction which establishes the geometry shown in Scheme 1.

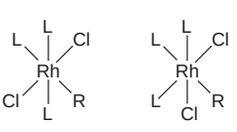

† Crystals of $[Rh(4\text{-}Bu^tpy)_3(CH_2Ph)Cl_2]$ **3a** have also been isolated but refinement of the X-ray data only resulted in a value of $R = 0.135$. Nevertheless, the refinement again indicated a *mer* arrangement of pyridine ligands.

Table 1 Selected bond lengths (Å) and angles (°) for complex **1b**

Rh–C(1)	2.045(10)	Rh–C(1)–Cl(3)	118.1(6)
Rh–N(1)	2.083(9)	C(1)–Rh–N(1)	88.5(4)
Rh–N(2)	2.041(9)	C(1)–Rh–N(3)	177.7(4)
Rh–N(3)	2.210(9)	C(1)–Rh–N(2)	91.2(4)
Rh–Cl(2)	2.340(3)	C(1)–Rh–Cl(2)	89.0(3)
Rh–Cl(3)	2.345(3)	C(1)–Rh–Cl(3)	92.8(3)
C(1)–Cl(1)	1.773(12)		

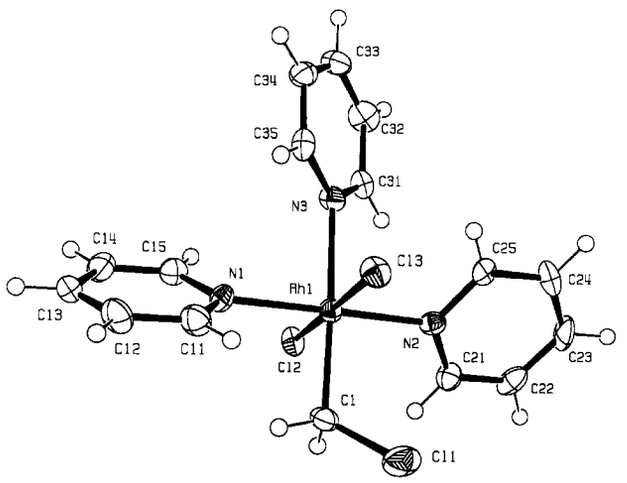

Fig. 1 Crystal structure of *mer*-$[Rh(py)_3(CH_2Cl)Cl_2]$ **1b**.

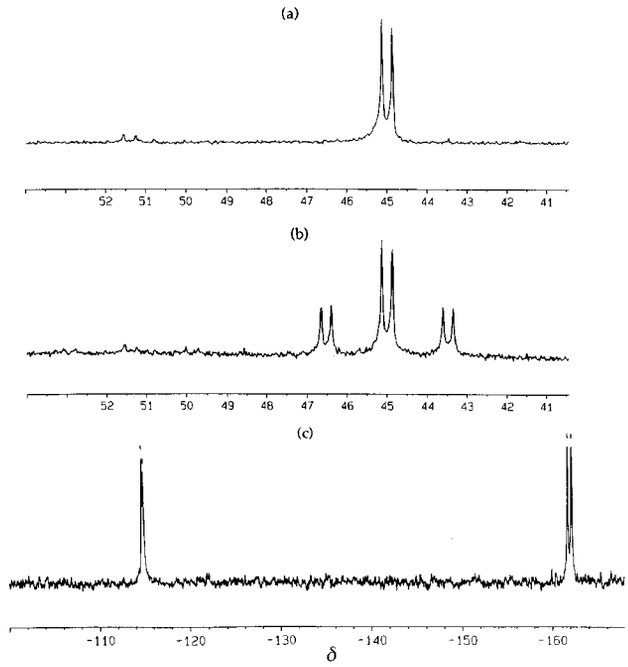

Fig. 2 The NMR spectra of *mer*-$[Rh(4\text{-}Bu^tpy)_3(CH_2Cl)Cl_2]$ **1a** in D_8-THF at −30 °C, (*a*) $^{13}C\text{-}\{^1H\}$, (*b*) ^{13}C and (*c*) $^{15}N\text{-}\{^1H\}$ INEPTRD.

X-Ray measurements

The crystal structure of *mer*-$[Rh(py)_3(CH_2Cl)Cl_2]$ **1b** has been determined (see Fig. 1) and found to adopt an octahedral geometry with the py ligands arranged in a *mer* environment. Selected bond lengths and angles for **1b** are given in Table 1.

Comparison of *d*(Rh–CH_2Cl) in complex **1b** with other rhodium(III) chloromethyl complexes show that the value of 2.045(10) Å for **1b** is similar to that observed for the chloromethyl complex $[RhCl(CH_2Cl)(edmp)_2]^+$ [2.050(7) Å; edmp = (2-aminoethyl)dimethylphosphine][14] and should be compared with the longest value which was found for $[RhCl(CH_2Cl)(dmpe)_2]Cl{\cdot}CH_2Cl_2$ [2.161(2) Å].[5] The different Rh–N bond lengths within **1b** reflect the influence of the *trans* ligand. Thus, *d*[Rh–N(1)] and *d*[Rh–N(2)] [2.083(9) and 2.041(9) Å respectively] are significantly shorter than *d*[Rh–N(3)] [2.210(9) Å], as a result of the strong *trans* influence of the CH_2Cl group. The values of *d*[Rh–N(1)] and *d*[Rh–N(2)] in **1b** are also similar to the Rh–N distances found in *mer*-$[Rh(py)_3Cl_3]$[22] which are shorter than those observed in other *mer*-$[M(py)_3Cl_3]$ analogues. For $[M(py)_3Cl_3]$ (M = Ti,[23] Fe,[24] Os[25] or Rh[22]) there is little variation in the values of *d*(M–Cl). The Rh–C–Cl bond angle [118.1(6)°] for **1b** falls within the range observed for other rhodium(III) chloromethyl complexes [115.3(4) and 119.9(7)°].

NMR measurements

The ^{13}C NMR measurements on the rhodium(III) complexes shown in Scheme 1 clearly establish that the predominant reaction involves oxidative addition of all these halogenated solvents, although it should be noted that a minor amount of *mer*-$[RhL_3Cl_3]$ is formed when L = Bu^tpy on reaction with the stoichometric amount of $CHCl_3$; this does not occur with either CH_2Cl_2 or $PhCH_2Cl$. Thus, for $[Rh(4\text{-}Bu^tpy)_3(CH_2Cl)Cl_2]$ **1a** both the $^{13}C\text{-}\{^1H\}$ [Fig. 2(a)] and ^{13}C spectra [Fig. 2(b)] show the presence of the $RhCH_2Cl$ group [δ(C) 45.0, ^1J(C–H) 152.9 Hz] and the different ^{13}C resonances associated with the pyridines (see Experimental section) all occur in the expected region with a relative intensity of 2:1. ^{15}N INEPT measurements on **1a** also show the presence of two resonances [Fig. 2(c)]. However, it is impossible to obtain accurate relative intensities from INEPT measurements but the ^{15}N resonance for **1a** at δ −114.9 [Fig. 2(c)] is both less intense and has a lower value of ^1J(Rh–N) (7.2 Hz) than the other resonance [δ(N) −162.0; ^1J(Rh–N) 17.7 Hz] and is consistent with 4-Bu^tpy being *trans* to the CH_2Cl group. However all the above NMR data, together with the observed 2:1 relative intensity of all the pyridine ^{13}C resonances (see Experimental section), do not readily allow the two possible isomers, **A** and **B**, to be distinguished, see above. Furthermore, there is little variation in either the values of δ(N) and ^1J(Rh–N) for pyridine *trans* to pyridine or *trans* to chloride as shown by measurements on *fac*- and *mer*-$[RhL_3Cl_3]$ (L = py or 4-Bu^tpy) (see Table 3). As a result, NMR measurements cannot distinguish **A** from **B** but, since only one isomer is formed, we feel that the structures adopted by **1a** in solution and the solid state are the same and the other rhodium(III) complexes shown in Scheme 1 probably adopt the same geometry.

The NMR data for all the rhodium(III) complexes shown in Scheme 1 are summarised in Table 2 and in the Experimental section and are entirely consistent with the proposed formulations. It should be noted that, because of the high *trans* effect of the R group, the ^{15}N resonance due to L *trans* to R disappears at room temperature probably because of rapid interexchange with the solvent (THF), whereas the ^{15}N resonance due to the *trans*-pyridines remains unchanged. Addition of >1 mol of CH_2Cl_2 or $CHCl_3$ per Rh atom (L = py) results in the exclusive formation of *mer*-$[Rh(py)_3Cl_3]$. It should be noted that ^{15}N NMR measurements on the product resulting from the preparation of $[RhL_3Cl_3]$ (L = 4-Bu^tpy) always show the presence of *fac*- and *mer*-$[RhL_3Cl_3]$ but refluxing in toluene (111 °C) results in the exclusive isomerisation of the *fac* to the more thermodynamically stable *mer* isomer.

Conclusion

This study has shown that facile oxidative addition of common solvents (*e.g.* CH_2Cl_2, $CHCl_3$ and $PhCH_2Cl$) occurs to give stable rhodium(III) adducts. The structure of *mer*-$[Rh(py)_3(CH_2Cl)Cl_2]$ has been determined by X-ray crystallography and NMR measurements are consistent with this configuration in solution. A possible mechanism for this reaction could involve the initial formation of $[RhL_3Cl]$ but attempts to spectro-

Table 2 The NMR data for $[RhL_3RCl_2]$ (L = py or 4-Bu^{t}py; R = CH_2Cl, $CHCl_2$ or CH_2Ph) at 243 K (see Scheme 1)

Complex	δ(C)[a]	^1J(Rh–C)[a]/Hz	$\delta(N_a)$[b]	$\delta(N_b)$[c]	^1J(Rh–N_a)[b]/Hz	^1J(Rh–N_b)[c]/Hz
1a *mer*-[Rh(4-Bu^{t}py)$_3$(CH_2Cl)Cl_2]	45.0	25.5	−162.0	−114.9	17.7	7.2
1b *mer*-[Rh(py)$_3$(CH_2Cl)Cl_2]	45.0	26.0	−157.4	−110.9	17.7	7.7
2a *mer*-[Rh(4-Bu^{t}py)$_3$($CHCl_2$)Cl_2]	73.6	34.0	−163.5	−124.7	17.9	8.7
2b *mer*-[Rh(py)$_3$($CHCl_2$)Cl_2]	71.7	32.7	−160.7	−119.8	18.0	8.5
3a *mer*-[Rh(4-Bu^{t}py)$_3$(CH_2Ph)Cl_2]	25.0	19.0	−161.4	−109.5	17.9	7.2

[a] Data for the RhCR′ group (R′ = H_2Cl, HCl_2 or H_2Ph). [b] N_a is *trans* to N-donor, L (L = py or 4-Bu^{t}py). [c] N_b is *trans* to R (R = CH_2Cl, $CHCl_2$ or CH_2Ph).

Table 3 ^{15}N NMR data for $[RhL_3Cl_3]$ (L = py or 4-Bu^{t}py)

Complex	$\delta(N_a)$[a]	$\delta(N_b)$[b]	^1J(Rh–N_a)[a]/ Hz	^1J(Rh–N_b)[b]/ Hz
mer-[Rh(4-Bu^{t}py)$_3Cl_3$]	−171.8	−163.7	16.6	17.3
fac-[Rh(4-Bu^{t}py)$_3Cl_3$]		−168.3		16.2
mer-[Rh(py)$_3Cl_3$]	−158.7	−148.5	17.7	19.5

[a] N_a is *trans* to the donor, L (L = py or 4-Bu^{t}py). [b] N_b is *trans* to Cl.

scopically identify this complex failed. This highly nucleophilic intermediate activates common solvents at room temperature towards oxidative addition to give the *mer*-rhodium(III) product but with an excess of RCl $[RhL_3Cl_3]$ is formed.

Experimental

The NMR measurements were carried out on a Bruker AMX200 or AMX400 spectrometer using commercial probes. ^{15}N-{^{1}H} NMR spectra were obtained on the AMX400 spectrometer using the INEPTRD (insensitive nuclei enhanced by polarisation transfer refocussed and decoupled) pulse sequence.[26] All spectra were recorded at −30 °C unless otherwise stated. Chemical shifts are quoted relative to internal $SiMe_4$ (^{13}C) and external $MeNO_2$ (^{15}N). All reactions were carried out under a nitrogen atmosphere using standard Schlenk-line techniques. Solvents were distilled under N_2 after reflux over CaH_2 (CH_2Cl_2, $CHCl_3$, $PhCH_2Cl$) or sodium–benzophenone (THF). Deuteriated solvents were dried over molecular sieves and stored under nitrogen. Pyridine and 4-*tert*-butylpyridine were used as received from Aldrich and $[Rh_2(C_8H_{14})_4(\mu\text{-}Cl)_2]$ was prepared using the literature method.[27]

Preparation of the complexes

[Rh(4-Bu^{t}py)$_3$(CH_2Cl)Cl_2] 1a. Dichloromethane (62.5 μl, 0.98 mmol) and 4-Bu^{t}py (432.5 μl, 2.94 mmol) were added to a suspension of $[Rh_2(C_8H_{14})_4(\mu\text{-}Cl)_2]$ (350 mg, 0.49 mmol) in THF (1 cm^3) to give a red solution. The solution was concentrated to give a yellow-orange solid (475 mg, 77%). This solid dissolved in D_8-THF (2 cm^3) to give a red solution and the species present was characterised by NMR spectroscopy (Found: C, 53.05; H, 6.6; N, 6.1. $C_{28}H_{41}Cl_3N_3Rh$ requires C, 53.5; H, 6.6; N, 6.7%). ^{13}C-{^{1}H} NMR (D_8-THF) with relative intensities of the 4-Bu^{t}py ligands in parentheses: δ(C) 163.6 (1) and 163.3 (2) (*p*-C), 156.7 (2) and 153.7 (1) (*o*-C), 123.7 (1) and 123.0 (2) (*m*-C), 36.8 (2) and 36.7 (1) (*ipso*-C), 31.8 (1) and 31.7 (2) (CH_3).

[Rh(py)$_3$(CH_2Cl)Cl_2] 1b. Pyridine (236.7 μl, 2.93 mmol) was added to a suspension of $[Rh_2(C_8H_{14})_4(\mu\text{-}Cl)_2]$ (350 mg, 0.49 mmol) in CH_2Cl_2–CD_2Cl_2 (3:1; 2 cm^3) to give a red solution of complex **1b** which was characterised by NMR spectroscopy. The formation of **1b** was immediate as evidenced by measuring the ^{13}C NMR spectrum at 243 K immediately after addition of reactants at room temperature. Yellow-orange crystals were obtained by layering this solution with light petroleum (bp 40–60 °C). ^{13}C NMR (CH_2Cl_2–CD_2Cl_2) with relative intensities of the py ligands in parentheses: δ(C) 155.4 (2) and 152.2 (1) (*o*-C), 138.7 (1) and 138.2 (2) (*p*-C), 125.5 (1) and 124.7 (2) (*m*-C).

[Rh(4-Bu^{t}py)$_3$($CHCl_2$)Cl_2] 2a. Chloroform (78.1 μl, 0.98 mmol) and 4-Bu^{t}py (432.5 μl, 2.94 mmol) were added to a suspension of $[Rh_2(C_8H_{14})_4(\mu\text{-}Cl)_2]$ (350 mg, 0.49 mmol) in THF (1 cm^3) to give a very deep red solution. The solution was concentrated to give a yellow-orange solid. This solid was then dissolved in D_8-THF (2 cm^3) to give a red solution and the species present were characterised by NMR spectroscopy. ^{13}C-{^{1}H} NMR (D_8-THF) with relative intensities of the 4-Bu^{t}py ligands in parentheses: δ(C) 164.5 (1) and 163.8 (2) (*p*-C), 157.0 (2) and 154.3 (1) (*o*-C), 123.7 (1) and 123.0 (2) (*m*-C), 36.8 (1) and 36.7 (2) (*ipso*-C), 31.8 (1) and 31.7 (2) (CH_3).

[Rh(py)$_3$($CHCl_2$)Cl_2] 2b. Pyridine (236.7 μl, 2.93 mmol) was added to a suspension of $[Rh_2(C_8H_{14})_4(\mu\text{-}Cl)_2]$ (350 mg, 0.49 mmol) in $CHCl_3$–CD_2Cl_2 (3:1; 2 cm^3) to give a very deep red solution. The species present in solution were characterised by NMR spectrosopy. ^{13}C NMR ($CHCl_3$–CD_2Cl_2) with relative intensities of the py ligands in parentheses: δ(C) 156.3 (2) and 152.7 (1) (*o*-C), 139.0 (1) and 138.8 (2) (*p*-C), 125.6 (1) and 125.0 (2) (*m*-C).

[Rh(4-Bu^{t}py)$_3$(CH_2Ph)Cl_2] 3a. Benzyl chloride (112.3 μl, 0.98 mmol) and 4-Bu^{t}py (432.5 μl, 2.94 mmol) were added to a suspension of $[Rh_2(C_8H_{14})_4(\mu\text{-}Cl)_2]$ (350 mg, 0.49 mmol) in THF (1 cm^3) to give a red solution. The solution was concentrated to give a yellow-orange solid (538 mg, 82%). This solid dissolved in D_8-THF (2 cm^3) to give a red solution and the species formed was characterised by NMR spectroscopy (Found: C, 60.7; H, 7.05; N, 6.0. $C_{34}H_{46}Cl_2N_3Rh$ requires C, 60.9; H, 6.9; N, 6.3%). ^{13}C-{^{1}H} NMR (D_8-THF) with relative intensities of the 4-Bu^{t}py ligands in parentheses: δ(C) 163.1 (1) and 162.4 (2) (*p*-C), 156.8 (2) and 153.7 (1) (*o*-C), 154.4 (*ipso*-C, $PhCH_2$), 131.8 (*o*-C, $PhCH_2$), 129.5 (*m*-C, $PhCH_2$), 124.8 (*p*-C, $PhCH_2$), 123.8 (1) and 122.6 (2) (*m*-C), 37.0 (1) and 36.8 (2) (*ipso*-C), 32.2 (1) and 32.1 (2) (CH_3).

Crystallography

Crystal data, data collection and processing details are given in Table 4. All data were recorded on a Rigaku AFC6S diffractometer at −120 °C using graphite-monochromatised Mo-Kα radiation, λ = 0.710 73 Å, 2θ–ω scans, $2\theta_{max}$ = 50°. An empirical absorption correction using ψ scans was applied by the TEXSAN system.

Structure analysis. The structure was refined by full-matrix least-square procedures on F^2.[28] All non-hydrogen atoms were treated as anisotropic and hydrogen atoms placed in geometric ideal positions and assigned isotropic thermal parameters 20%

Table 4 Crystal structure analysis, crystal data and experimental details for complex **1b**

Formula	$C_{16}H_{17}Cl_3N_3Rh$
M	460.59
Appearance	Yellow prism
Space group	$P2_1/c$
Crystal system	Monoclinic
a/Å	13.103(6)
b/Å	8.238(4)
c/Å	16.808(5)
β/°	100.21(4)
U/Å^3	1785.6(13)
Z	4
D_c/g cm^{-3}	1.713
F(000)	920
μ(Mo-Kα)/cm^{-1}	14.06
Crystal dimensions/mm	0.25 × 0.25 × 0.20
Reflections measured	3194
Unique reflections	3051
T_{max}, T_{min}	1.00, 0.872
R [$I > 2\sigma(I)$]	0.068
$wR2$ (all data)	0.190
Final difference electron density (maximum, minimum)/e Å^{-3}	1.38, −1.35

greater than the B equivalent value of the atom to which they were bonded.

CCDC reference number 186/1349.

See http://www.rsc.org/suppdata/dt/1999/1109/ for crystallographic files in .cif format.

Acknowledgements

We thank EPSRC for a studentship (to K. J. B.) and the Leverhulme Trust for the award of a Research Fellowship (to B. T. H.).

References

1 J. Chang and R. G. Bergman, *J. Am. Chem. Soc.*, 1987, **109**, 4298.
2 D. A. Freedman and K. R. Mann, *Inorg. Chem.*, 1991, **30**, 836.
3 W. L. Olson, D. A. Nagaki and L. F. Dahl, *Organometallics*, 1986, **5**, 630.
4 O. J. Scherer and H. Jungmann, *J. Organomet. Chem.*, 1981, **208**, 153.
5 T. B. Marder, W. C. Fultz, J. C. Calabrese, R. L. Harlow and D. Milstein, *J. Chem. Soc.*, *Chem. Commun.*, 1987, 1543.
6 P. Leoni, *Organometallics*, 1993, **12**, 2432.
7 W. A. Herrmann, C. Broßmer, T. Priermeier and K. Öfele, *J. Organomet. Chem.*, 1994, **481**, 97.
8 P. J. Fennis, P. H. M. Budzelaar, J. H. G. Frijns and A. G. Orpen, *J. Organomet. Chem.*, 1990, **393**, 287.
9 C. A. Ghilardi, S. Midollini, S. Moneti, A. Orlandini and J. A. Ramirez, *J. Chem. Soc.*, *Chem. Commun.*, 1989, 304.
10 P. K. Monaghan and R. J. Puddephatt, *Organometallics*, 1985, **4**, 1406.
11 H. Nishiyama, M. Horihata, T. Hirai, S. Wakamatsu and K. Itoh, *Organometallics*, 1991, **10**, 2706.
12 H. F. Haarman, J. M. Ernsting, M. Kranenburg, H. Kooijman, N. Veldman, A. L. Spek, P. W. N. M. van Leeuwen and K. Vrieze, *Organometallics*, 1997, **16**, 887.
13 T. Yoshida, T. Ueda, T. Adachi, K. Yamamoto and T. Higuchi, *J. Chem. Soc.*, *Chem. Commun.*, 1985, 1137.
14 K. Kashiwabara, A. Morikawa, T. Suzuki, K. Isobe and K. Tatsumi, *J. Chem. Soc.*, *Dalton Trans.*, 1997, 1075.
15 R. Ziessel, L. Toupet, S. Chardon-Noblat, A. Deronzier and D. Matt, *J. Chem. Soc.*, *Dalton Trans.*, 1997, 3777.
16 E. G. Burns, S. S. C. Chu, P. de Meester and M. Lattman, *Organometallics*, 1986, **5**, 2383.
17 G. E. Ball, W. R. Cullen, M. D. Fryzuk, B. R. James and S. J. Rettig, *Organometallics*, 1991, **10**, 3767.
18 J. Brunet, X. Couillens, J. Daran, O. Diallo, C. Lepetit and D. Neibecker, *Eur. J. Inorg. Chem.*, 1998, 349.
19 M. A. Curiano, M. A. Tena and L. A. Oro, *J. Chem. Soc.*, *Chem. Commun.*, 1992, 2123.
20 M. Oliván and K. G. Caulton, *Chem. Commun.*, 1997, 1733.
21 H. B. Friedrich and J. R. Moss, *Adv. Organomet. Chem.*, 1991, **33**, 235.
22 K. R. Acharya, S. S. Tavale and T. N. Guru Row, *Acta Crystallogr.*, *Sect. C*, 1984, **40**, 1327.
23 R. K. Collins and M. G. B. Drew, *Inorg. Nucl. Chem. Lett.*, 1972, **8**, 975.
24 A. Hoser, Z. Kaluski, M. Januszczyk, J. Pietrzak and T. Glowiak, *Acta. Crystallogr.*, *Sect. C*, 1983, **39**, 1039.
25 A. J. Blake, G. A. Heath, G. Smith, L. J. Yellowlees and D. W. A. Sharp, *Acta Crystallogr.*, *Sect. C*, 1988, **44**, 1836.
26 O. W. Sørensen and R. R. Ernst, *J. Magn. Reson.*, 1983, **51**, 477.
27 A. van der Ent and A. L. Onderdelinden, *Inorg. Synth.*, 1973, **14**, 93.
28 G. M. Sheldrick, SHELXL 97, Program for X-Ray Structure Determination, Göttingen, 1997.

Paper 8/09652J